

## Domain wall configuration and magneto-transport properties in dual spin-valve with nanoconstriction

Byong Sun Chun, Han-Chun Wu, Su Jung Noh, In Chang Chu, Santiago Serrano-Guisan et al.

Citation: *Appl. Phys. Lett.* **100**, 242409 (2012); doi: 10.1063/1.4729126

View online: <http://dx.doi.org/10.1063/1.4729126>

View Table of Contents: <http://apl.aip.org/resource/1/APPLAB/v100/i24>

Published by the AIP Publishing LLC.

---

### Additional information on *Appl. Phys. Lett.*

Journal Homepage: <http://apl.aip.org/>

Journal Information: [http://apl.aip.org/about/about\\_the\\_journal](http://apl.aip.org/about/about_the_journal)

Top downloads: [http://apl.aip.org/features/most\\_downloaded](http://apl.aip.org/features/most_downloaded)

Information for Authors: <http://apl.aip.org/authors>

## ADVERTISEMENT

### High-Voltage Amplifiers

Voltage Range from  $\pm 50\text{V}$  to  $\pm 60\text{kV}$   
Current to 25A

### Electrostatic Voltmeters

Contacting & Non-Contacting  
Measure to 20kV - Sensitive to 1mV



ENABLING RESEARCH AND  
INNOVATION IN DIELECTRICS,  
ELECTROSTATICS, MATERIALS,  
PLASMAS AND PIEZOS



[www.trekinc.com](http://www.trekinc.com)

TREK, INC. • 11601 Maple Ridge Road, Medina, NY 14103 USA • Toll Free in USA 1-800-FOR-TREK • (t)+1-585-798-3140 • (f)+1-585-798-3106 • sales@trekinc.com

## Domain wall configuration and magneto-transport properties in dual spin-valve with nanoconstriction

Byong Sun Chun,<sup>1</sup> Han-Chun Wu,<sup>2</sup> Su Jung Noh,<sup>3</sup> In Chang Chu,<sup>4</sup> Santiago Serrano-Guisan,<sup>5</sup> Chanyong Hwang,<sup>1</sup> Igor V. Shvets,<sup>2</sup> Zhi-Min Liao,<sup>2</sup> Mohamed Abid,<sup>6,7,a)</sup> and Young Keun Kim<sup>3,a)</sup>

<sup>1</sup>Division of Industrial Metrology, Korea Research Institute of Standards and Science, Daejeon, South Korea

<sup>2</sup>CRANN, School of Physics, Trinity College Dublin, Dublin 2, Ireland

<sup>3</sup>Department of Materials Science and Engineering, Korea University, Seoul 136-713, Korea

<sup>4</sup>Global EMI/EMC Team, 3 M Korea Innovation Center, Hwaseong-Si, Korea

<sup>5</sup>Physikalisch-Technische Bundesanstalt, Bundesallee 100, 38116 Braunschweig, Germany

<sup>6</sup>Ecole Polytechnique Federale de Lausanne/IPMC/LPMN, Station 3, CH 1015, Switzerland

<sup>7</sup>King Saud University, Riyadh 11451, Saudi Arabia

(Received 15 March 2012; accepted 26 May 2012; published online 13 June 2012)

We investigated the effect of external field on magneto-transport properties of synthetic antiferromagnet dual spin-valve with nanoconstriction with focus on domain wall (DW) configuration and magnetization reversal process. As magnetic field rotated from in-plane to out-of-plane along hard axis configuration, the magnetization reversal mode changed from a vortex to a transverse type, and a multistep switching process appeared due to the development of a transverse magnetization reversal mode with DW pushing towards the higher anisotropy region. The difference in the shape of nanoconstriction made an asymmetric energy barrier to the DW propagation which resulted in an asymmetry depinning field. © 2012 American Institute of Physics. [<http://dx.doi.org/10.1063/1.4729126>]

Ferromagnetic nanostructures have attracted a lot of attention in fundamental physics. They also possess potential for applications to numerous devices, such as logic and memory devices.<sup>1,2</sup> In those devices, data can be stored in the form of a magnetic domain wall (DW). Theoretical study has shown that a DW can be formed in the contact region when the electrodes are magnetized antiparallel to each other.<sup>3,4</sup> The key issue to effectively implement this idea for memory device is to manipulate the DW configurations in a reproducible and reliable way. Much effort has been devoted to manipulate the DW by a magnetic field or by a spin polarized current through spin transfer torque.<sup>5,6</sup> One of the most established DW control methods is to place notches in the magnetic nanowire and multilayer, as the DWs are pinned at the notches due to a lower energy.<sup>7</sup> Another method is to place a nanoconstriction, where the DW becomes geometrically constrained.<sup>4</sup> It is well known that the presence of a pinned DW in such a nanostructure can be probed by measuring the magnetoresistance (MR), which is sensitive to the relative magnetization of the two wires.

The effect of a magnetic DW on the magneto-transport properties on the nanostructured spin-valves (SVs) is currently a topic of great interest; therefore, further understanding of the magneto-transport properties relating to the SV with nanoconstriction is highly important. Moreover, the nanoconstriction shape is a key parameter for the formation of DW configuration and width.<sup>8</sup> Up to now, studies of the effect of a DW on the magneto-transport properties have been based on the simple structure such as a single SV and a nanowire composed of a single layer.

Here, in this letter, we take complicated systems such as synthetic antiferromagnet-based dual spin-valve (SAF-DSV) structure (i.e., the SV structure is doubled symmetrically with respect to the ferromagnetic layer) to control the effect of a DW on the magneto-transport properties. We demonstrate the effect of the direction of the applied magnetic field with respect to nanoconstriction shapes on the magneto-transport properties including DW configuration and reversal process. Using this method, as magnetic field rotated from an in-plane along easy axis configuration to an out-of-plane along hard axis configuration, the magnetization reversal mode changed from a vortex to a transverse type, and a multistep switching process appeared. The multistep switching in the MR curves is due to the contribution of higher pressure and development of transverse magnetization reversal mode when the sweep field along perpendicular to the sample axis with DW pushing towards the higher anisotropy region. Our systematic experiments also show that an asymmetric depinning field in the SAF-DSV is related to an asymmetric energy barrier to domain wall propagation as well as the difference in DW width at the nanoconstriction.

The SAF-DSV structure in this study was of the form; Si/SiO<sub>2</sub>/Ta 5/CoFe 3/Cu 3/[CoFe 1.7/Ru 0.3/CoFe 5.5]SAF/Cu 2.8/CoFe 5/Cu 2.8/CoFe 1.5/IrMn 10/Ta 5 (thickness in nm), where the CoFe 1.7/Ru 0.3/CoFe 5.5 trilayer is SAF. Samples were prepared using a six-target dc magnetron sputtering system under a typical base pressure of less than  $2 \times 10^{-7}$  Torr. The MR of the non-nanoconstricted and nanoconstricted SV structures was characterized using a physical property measurement system (PPMS) by Quantum Design. Device fabrication was carried out using e-beam lithography employing a negative-tone ma-N 2403 resist and Ar<sup>+</sup> ion etching. Subsequently, after removal of the resist, UV lithography patterning was performed to fabricate the macroscopic

<sup>a)</sup>Authors to whom correspondence should be addressed. Electronic addresses: ykim97@korea.ac.kr and mohamed.abid@epfl.ch.

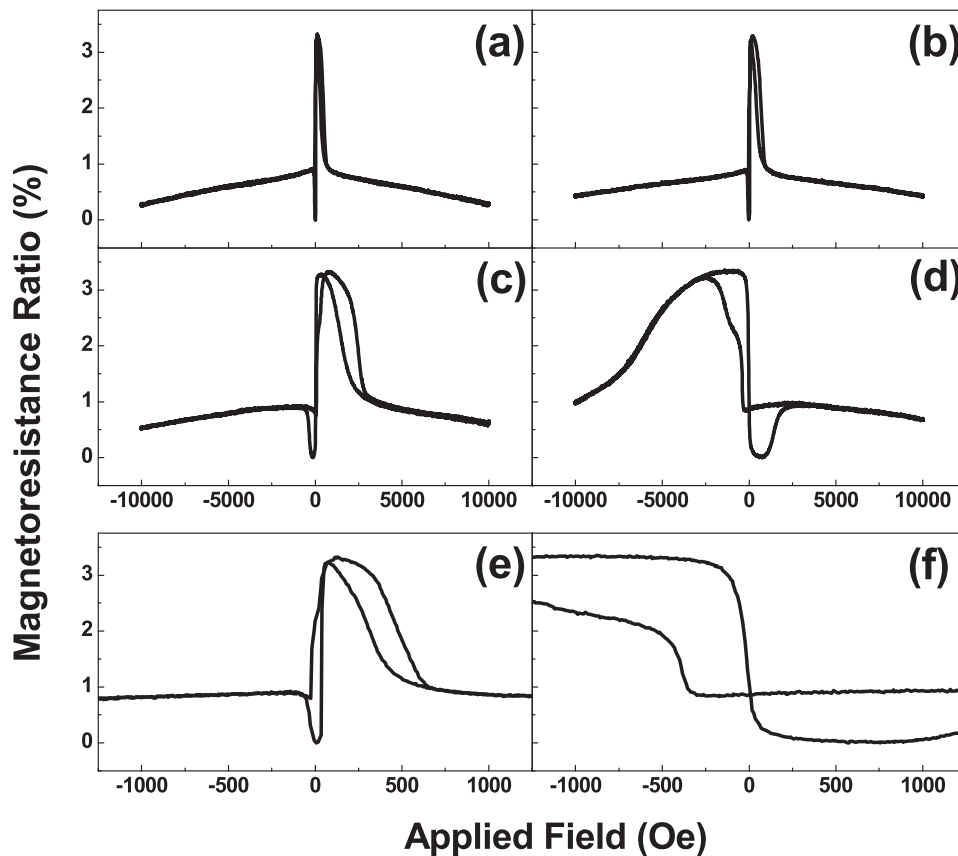


FIG. 1. Magneto-transport curves without a nanoconstriction as the sweep field along (a) the easy direction, (b) 30°, (c) 60°, and (d) perpendicular to the sample axis. Minor magneto-transport curves with the sweep field along the (e) easy and (f) perpendicular direction to the sample axis.

metal contacts. In order to interpret the experimental data, we have employed a micromagnetic modeling study based on the Landau–Lifschitz–Gilbert (LLG) equation solver. Calculation parameters such as polarization of 0.4, and exchange stiffness of  $1.05 \times 10^{-6}$  erg/cm were used. The unit vector size was  $3.5 \text{ nm} \times 3.5 \text{ nm}$ . The time step was  $4.74 \times 10^{-3}$  ps and conversion was set at  $1 \times 10^{-5}$  for calculation.

Figure 1 depicts the magneto-transport properties of the SAF-DSV structure without a nanoconstriction as the sweep field from an in-plane along easy axis configuration ( $0^\circ$ ) to an out-of-plane along hard axis configuration ( $90^\circ$ ), with  $30^\circ$  rotation step to the sample axis. One can see from Fig. 1 that, as the sweep field is rotated away from the easy direction, the coercivity field ( $H_c$ ) increases, followed by a sharp decrease when the applied field is in the perpendicular direction to the sample axis (Fig. 1(d)).

It is known that the dependence of  $H_c$  on the angle between the applied field direction and the easy axis is closely correlated with the magnetization reversal mode; different reversal modes would be expected to show different trends in the angular dependence of  $H_c$ .<sup>9</sup> There are usually three reversal modes.<sup>9–11</sup> First, the vortex mode, magnetic moments incoherently rotate in a curling pattern via propagation of a vortex domain wall. Second, the transverse mode, magnetic moments rotate progressively via propagation of a transverse domain wall. Third, the coherent rotation, all magnetic moments coherently rotate in unison. It has been reported that the  $H_c$  increases in the vortex mode, but decreases in the transverse mode with increasing angle between the applied field direction and easy axis of the sample.<sup>11,12</sup> As shown in this figure, an increase in  $H_c$  has been clearly observed with increasing angle from  $0^\circ$  to  $60^\circ$ , indicating a vortex mode. While further increasing the angle

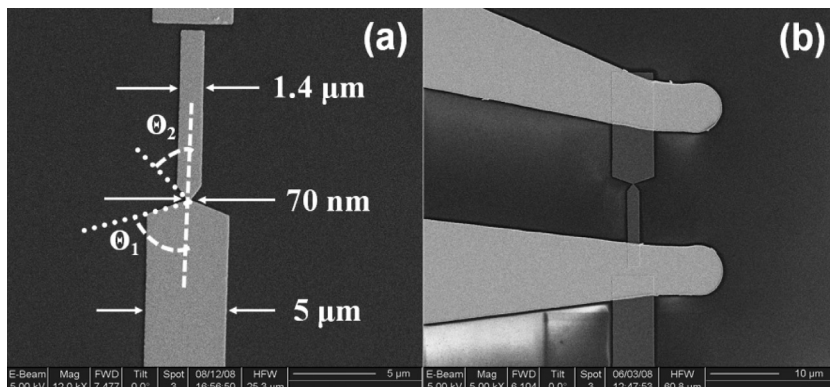


FIG. 2. A SEM image of a (a) patterned device<sup>16</sup> and (b) two electrodes for measurement of magneto-transport properties.

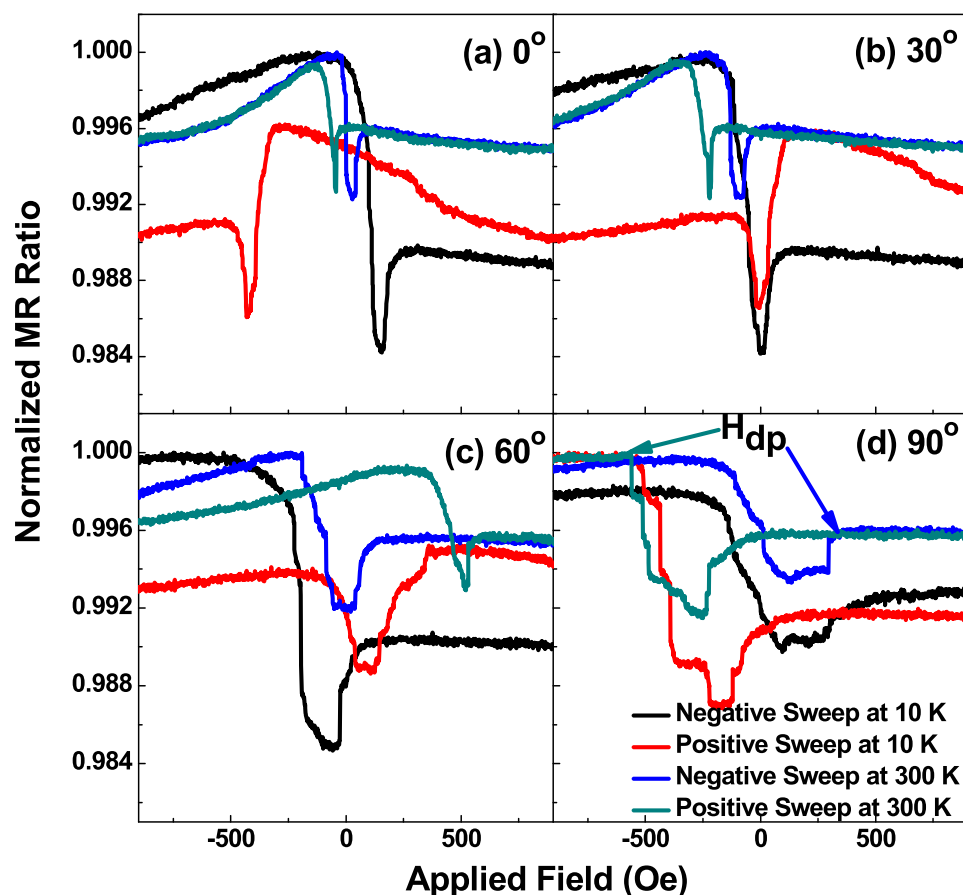


FIG. 3. Minor magneto-transport curves with a nanoconstriction as the sweep field along the (a) easy direction, (b) 30°, (c) 60°, and (d) perpendicular to the sample axis.

from 60° to 90°,  $H_c$  decreases suggesting a change in the magnetization reversal from a vortex type to a transverse mode beyond 60°.

The spin flop process also studied, where the pinning direction cants largely from the easy axis. As the sweep field is rotated away from the easy direction, the MR curves show an increase of exchange bias field ( $H_{\text{exB}}$ ). In particular, when the field is applied perpendicular to the sample, an opposite exchange bias is observed which indicates that the pinned direction of SAF layer is almost perpendicular to the easy axis of the CoFe 5 nm free layer. It was theoretically predicted that in a SAF structure spin flop can occur under an external magnetic field.<sup>13</sup> It was experimentally observed that the spin flop of a SAF structure was induced by the magnitude of the magnetic annealing field<sup>14</sup> and the thickness difference of two magnetic layers in the pinned SAF.<sup>15</sup> Thus, the pinned direction of the SAF could be canted and these angular dependences of the magneto-transport properties are largely due to the spin flop effect of the SAF.

Figures 1(e) and 1(f) display the minor magneto-transport curves of the SAF-DSV structure without a nanoconstriction as the sweep field along the easy direction and perpendicular direction to the sample axis, respectively. A detailed description of these figures will be discussed including Fig. 3.

Figure 2 shows scanning electron microscope (SEM) images of a typical structure used in this study (top view). As shown in Fig. 2(a), our nanoconstricted SAF-DSV structure is composed of two pads (large and small rectangle) with nanoconstriction. The difference in the pad size is pro-

posed to facilitate a magnetic configuration, where a DW is formed at the constriction due to the shape anisotropy at which the magnetization in the pads switches.<sup>16</sup> To trap a DW, a V-shaped nanoconstriction with a size of 40 nm is located in the middle of two pads with different widths. The pads have two electrodes made of nonmagnetic material, 35 nm-thick Au, for measurement of magneto-transport properties (Fig. 2(b)).

Figure 3 displays minor magneto-transport curves of the nanoconstricted SAF-DSV with different magnetic field directions at 10 K and 300 K. One can see from Fig. 3 that jumps and kinks are clearly observed. Since the device without nanoconstriction does not show any noticeable jumps or kinks (in Figs. 1(e) and 1(f)), the observed jump and kink in the MR curves originate from the contributions of pinning and depinning DWs at the nanoconstriction.

Most interestingly, as the sweep field is rotated away from the easy direction (Figs. 3(b)–3(d)) with DW pushing towards the higher anisotropy region (in our case, positive sweep), more kinks and jumps are observed in the MR curves compared to that of sweep field is applied in-plane to the sample (Fig. 3(a)) with DW pushing towards the lower anisotropy region (in our case, negative sweep).

It was theoretically predicted that under the strong enough magnetic field, the internal structure of a moving DW periodically transforms between the vortex and transverse wall configurations.<sup>17,18</sup> At low field, the DW shows a viscous motion with a high velocity proportional to the applied magnetic field. Above a critical (so-called Walker breakdown) field, however, the DW shows an oscillation

motion with a slow drifting in the applied field direction. These dynamic transformations are resulted from the serial process of the creation, propagation, and annihilation of DWs with the conservation of total topological charges. Transverse DW has the simplest structure. The results of the micromagnetic simulation showed that the core region in the transverse wall was magnetized perpendicular to the wire length, which would be the expected configuration if there was any misalignment between the field direction and the length of the wire, leading to an in-plane field component perpendicular to the wire.<sup>19</sup> If the sweep field is rotated away from the easy direction, as previously mentioned in Fig. 1, the magnetization reversal mode changes from a vortex to a transverse mode.

The field is efficient in moving the DW into the lower anisotropy region. As shown in Fig. 2, the  $1.4\ \mu\text{m}$  width pad has a high shape anisotropy compared to that with a  $5\ \mu\text{m}$  width one. When pushing the DW towards the higher anisotropy region (positive sweep), a higher pressure is exerted on the DW until depinning of the DW.<sup>20</sup> When pushing the DW towards the lower anisotropy region (negative sweep), however, a relatively lower pressure is exerted on the DW. Therefore, more kinks and jumps in the MR curves are due to the contribution of higher pressure and development of transverse magnetization reversal mode when the sweep field along perpendicular to the sample axis with DW pushing towards the higher anisotropy region.

Figure 3 also shows different depinning field ( $H_{\text{dp}}$ ) for positive sweep and negative sweep. The  $H_{\text{dp}}$  is inversely proportional to the domain wall width ( $\delta = \pi \sqrt{A/K}$ ), where  $A$  and  $K$  are the exchange stiffness and the anisotropy constant, respectively. According to the micromagnetic modeling study, the DW width appeared to be greatly affected by the shape of the nanoconstriction (i.e., the angles ( $\Theta_{1,2}$ ) between the x-axis and the edge of the wire).<sup>8</sup> To reduce the magneto-static energy, the magnetic moments generally tend to align parallel to the edges. If the angle between the nearest neighbor spin moments in the constriction becomes smaller (in our case  $\Theta_2$ , see Fig. 2), the DW width becomes wider. For a larger angle (in our case,  $\Theta_1$ ), the magnetic moments near the constriction align in a direction perpendicular to the plane and; as a consequence, the DW width becomes narrower. The DW ejects from a  $5\ \mu\text{m}$  width pad with larger angle  $\Theta_1$  (red and cyan curves, positive sweep), and therefore, has higher  $H_{\text{dp}}$  than the DW ejects from a  $1.4\ \mu\text{m}$  width pad with lower angle  $\Theta_2$  (black and blue curves, negative sweep). It is clear that the difference in the shape of the nanoconstriction makes an asymmetric energy barrier to DW propagation that leads to an asymmetry in the DW depinning forces.<sup>21</sup>

Figure 4 shows the calculated results of the DW configuration at the remanent states in the constricted region corresponding to the field applied to (a) easy and (b) perpendicular direction to the sample axis. As shown in this figure, the applied field direction to the sample axis plays an important role in the formation of DW. When the field is applied to (a) easy or (b) perpendicular direction to the sample axis, the results show that the DW formed in the nanoconstricted region is in a vortex mode or in a transverse mode, respectively. As previously mentioned in the Fig. 1,

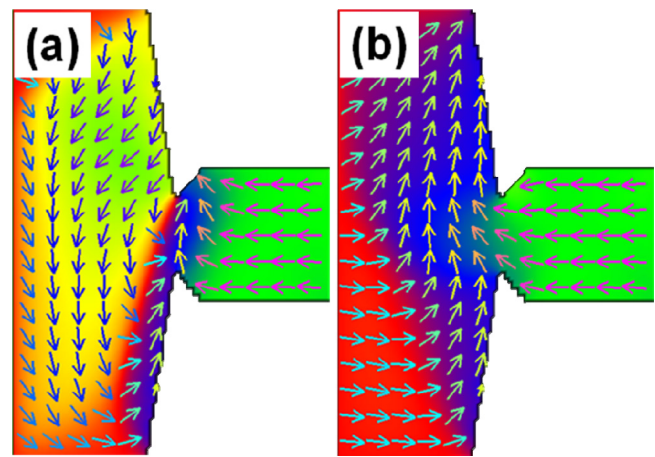


FIG. 4. Spin configuration for nanoconstriction with different applied field direction to the sample axis. When the field was applied to the easy and perpendicular direction to the sample axis, (a) a vortex and (b) a transverse DW was observed in the nanoconstricted region.

magnetization reversal occurs in a vortex mode then changes to a transverse mode when the applied field direction to the sample axis is beyond  $60^\circ$ . Therefore, our experimental results agree well with the simulation results.

In summary, we present the effect of the direction of the applied magnetic field with respect to nanoconstriction shapes on the magneto-transport properties including DW configuration and reversal process using a SAF-DSV structure. We can control the DW configuration and reversal process from a vortex to a transverse type by changing the applied field direction to the nanoconstricted SAF-DSV. The multistep switching in the MR curves is due to the contribution of higher pressure and development of transverse magnetization reversal mode when the sweep field along perpendicular to the sample axis with DW pushing towards the higher anisotropy region. Our results also showed an asymmetric depinning field. The difference in the shape of nanoconstriction makes an asymmetric energy barrier to domain wall propagation due to the difference in the DW width, which leads to an asymmetry in the domain wall depinning forces.

This work was supported by the National Research Foundation of Korea (2011-0016497 and 2010-359-D00033) and by the International Research & Development Program of the National Research Foundation of Korea (NRF) funded by the Ministry of Education, Science and Technology (MEST) of Korea (Grant No. 2011-00127). H.C.W. and I.V.S. acknowledge the financial support from SFI under Contract No. 06/IN.1/I91. M.A. acknowledges the financial support from NPST (No.11-NAN1466-02).

<sup>1</sup>D. A. Allwood, G. Xiong, M. D. Cooke, C. C. Faulkner, D. Atkinson, N. Vernier, and R. P. Cowburn, *Science* **296**, 2003 (2002).

<sup>2</sup>S. S. P. Parkin, M. Hayashi, and L. Thomas, *Science* **320**, 190 (2008).

<sup>3</sup>G. Tatara, Y. W. Zhao, M. Muñoz, and N. García, *Phys. Rev. Lett.* **83**, 2030 (1999).

<sup>4</sup>P. Bruno, *Phys. Rev. Lett.* **83**, 2425 (1999).

<sup>5</sup>L. Berger, *J. Appl. Phys.* **71**, 2721 (1992).

<sup>6</sup>J. Slonczewski, *J. Magn. Mater.* **159**, L1 (1996).

<sup>7</sup>A. J. Zambano and W. P. Pratt, *Appl. Phys. Lett.* **85**, 1562 (2004).

<sup>8</sup>S. D. Kim, B. S. Chun, and Y. K. Kim, *J. Appl. Phys.* **101**, 09F504 (2007).

- <sup>9</sup>J. Escrig, J. Bachmann, J. Jing, M. Daub, D. Altbir, and K. Nielsch, *Phys. Rev. B* **77**, 214421 (2008).
- <sup>10</sup>P. Landeros, S. Allende, J. Escrig, E. Salcedo, D. Altbir, and E. E. Vogel, *Appl. Phys. Lett.* **90**, 102501 (2007).
- <sup>11</sup>O. Albrecht, R. Zierold, S. Allende, J. Escrig, C. Patzig, B. Rauschenbach, K. Nielsch, and D. Gorlitz, *J. Appl. Phys.* **109**, 093910 (2011).
- <sup>12</sup>L. Sun, Y. Hao, C. L. Chien, and P. C. Searson, *IBM J. Res. Dev.* **49**, 79 (2005).
- <sup>13</sup>J. G. Zhu, *IEEE Trans. Magn.* **35**, 655 (1999).
- <sup>14</sup>H. C. Tong, C. Qian, L. Miloslavsky, S. Funada, X. Shi, F. Liu, and S. Dey, *J. Appl. Phys.* **87**, 5055 (2000).
- <sup>15</sup>S. H. Jang, T. Kang, H. J. Kim, and K. Y. Kim, *J. Magn. Magn. Mater.* **239**, 179 (2002).
- <sup>16</sup>S. J. Noh, B. S. Chun, H. C. Wu, I. V. Shvets, I. C. Chu, M. Abid, S. Serano-Guisan, and Y. K. Kim, *IEEE Trans. Magn.* **47**, 2436 (2011).
- <sup>17</sup>O. A. Tretiakov, D. Clarke, G.-W. Chern, Ya. B. Bazaliy, and O. Tchernyshyov, *Phys. Rev. Lett.* **100**, 127204 (2008).
- <sup>18</sup>D. J. Clarke, O. A. Tretiakov, G.-W. Chern, Ya. B. Bazaliy, and O. Tchernyshyov, *Phys. Rev. B* **78**, 134412 (2008).
- <sup>19</sup>G. X. Miao, M. D. Mascaró, C. H. Nam, C. A. Ross, and J. S. Moodera, *Appl. Phys. Lett.* **99**, 032501 (2011).
- <sup>20</sup>A. Ruotolo, A. Oropallo, F. M. Granozio, G. P. Pepe, P. Perna, U. S. di Uccio, and D. Pullini, *Appl. Phys. Lett.* **91**, 132502 (2007).
- <sup>21</sup>D. A. Allwood, G. Xiong, and R. P. Cowburn, *Appl. Phys. Lett.* **85**, 2848 (2004).